RSC Advances

ROYAL SOCIETY OF CHEMISTRY

www.rsc.org/advances

In this review, we specially highlight the recent research efforts toward understanding the defect chemistry of titanium dioxide—a widely-studied multifunctional metal oxide. Particular attention is paid to the synthesis of self-modified TiO_2 materials with Ti^{3+}/oxygen vacancies and the favorable effects of these defects on properties and applications of the obtained materials.

ARTICLE TYPE

Self-modification of titanium dioxide materials by Ti³⁺ and/or oxygen vacancies: new insights into defect chemistry of metal oxides

Juan Su,[a] Xiaoxin Zou*[b] and Jie-Sheng Chen*[a]

Defect chemistry of metal oxides is a very important research aspect of inorganic solid-state materials. This is because (i) a certain amount of defects or imperfections are always present in the metal oxide materials; (ii) the presence of the defects affect, even determine sometimes, the physical and chemical properties of materials; (iii) more importantly, defects do not necessarily have adverse effects on the

10 properties of materials, and judicious "defect engineering" can bring about improved properties desired in a material system, and even some new useful functionalities that are not available to the "perfect" material. In this review, we specially highlight the recent research efforts toward understanding the defect chemistry of titanium dioxide (also known as titania, TiO_2)—a widely-studied multifunctional metal oxide. In the discussion, particular attention is paid to *the synthesis of Ti³⁺/oxygen vacancies self-modified*

15 *TiO_2 materials* and the *favorable effects of these defects* on materials' properties and applications. This review, focusing on a representative metal oxide (*i.e.*, TiO_2), is anticipated to provide some new insights into general defect chemistry of metal oxides, and to give an impetus on the development of "defect engineering" of metal oxide materials.

1. Introduction

20 Titanium (Ti) is the *ninth* most abundant element (0.63%) in the Earth's crust, and it is only exceeded by O, Si, Al, Fe, Ca, Na, K and Mg in terms of the abundance of elements.[1] As the most important oxide of titanium, titanium dioxide (also known as titania, TiO_2), which mainly exists in three polymorphs (*i.e.*,

25 anatase, rutile and brookite), is a multifunctional metal oxide material.[2-8] Since the early twentieth century, TiO_2 material has been commercially used as white pigment and sunscreen additive etc. These conventional applications of TiO_2 material mainly benefit from its basic physical and chemical properties, such as

30 high refractive index, strong UV-light absorbing capabilities, excellent chemical stability and earth-abundant feature.[2-8]

In 1972, Fujishima and Honda discovered that the water splitting took place on a TiO_2 electrode under ultraviolet (UV) light irradiation.[9] This pioneering work immediately excited great

35 interest among chemical researchers and simultaneously enormous efforts were devoted to the research of TiO_2 material.[1-8] This has resulted in many promising TiO_2-based applications, ranging from photovoltaics, photocatalysis and self-cleaning techniques to sensors and photo-/electrochromics.[1-15] The TiO_2

40 material is generally the most core component in these applications, and the properties of TiO_2 material mainly determine the efficiency of these applications, and their operating circumstances we finally use. Thus, judiciously tuning the structure of TiO_2 material to optimize its properties/functions and

45 further understanding the structure–property/function correlations have been actively pursued.

The main structure parameters of TiO_2 material, which are

strongly related to its properties/functions, typically includes crystal phase, crystallinity, shape, size, surface structure and

50 defects.[16-20] While many strategies were developed to optimize the properties/functions of TiO_2 material by tuning its crystal phase, crystallinity, shape, size, and/or surface structure, the defect tuning of TiO_2 material maintained elusive for a long time. However, recently continued breakthroughs have been made in

55 the synthesis and applications of TiO_2 materials with a large amount of defects (*i.e.*, Ti³⁺ and oxygen vacancies); and especially the favorable effects of these defects on materials' properties have been attracted wide attention.

In this review, the defects in TiO_2 are particularly designated

60 as Ti³⁺ ions and oxygen vacancies; and the method that is used to create these defects in TiO_2 are named as "self-modification". The most important characteristic of the self-modification method is that the improvement of TiO_2 property is originated from the deliberately-introduced defects in it. In other words, through

65 modifying the atomic structures of TiO_2 by the deliberately-introduced defects (*e.g.*, missing or rearranging titanium/oxygen atoms), the properties of TiO_2 can be enhanced to a great extent. Herein we summarize recent development in the synthesis of self-modified TiO_2 materials with Ti³⁺ ions and/or oxygen vacancies,

70 and the favorable effects of these defects on materials' properties and applications.

2. Synthetic strategies for self-modified TiO_2

The synthetic strategies to self-modified TiO_2 can be roughly divided into categories: "partial reduction method" and "partial

75 oxidation method". The former is more frequently used to prepare

self-modified TiO_2 materials.

X-ray photoelectron (XPS) and electron paramagnetic resonance (EPR) spectroscopies are generally applied to study the Ti^{3+} ions and oxygen vacancies in TiO_2. XPS is an effective technique to determine the presence and amount of Ti^{3+} ions in TiO_2, but it cannot give any information about oxygen vacancies. In addition, because the detection depth of the XPS measurement is < 10 nm, XPS measurement can only provide the structural information of Ti^{3+} species at the surface and subsurface of the TiO_2 particles. As a complementary technique of XPS, EPR can give some valuable information about Ti^{3+} species and single-electron-trapped oxygen vacancies (V_o˙), EPR can quantitatively analyse Ti^{3+} and V_o˙ using 2-diphenyl-1-picrylhydrazyl (DPPH) and a manganese (Mn) marker as the standards.

It is worth noting that the relationships between Ti^{3+} and oxygen vacancy are very complex in a solid TiO_2 material. There are mainly three situations: (1) when the electric charges of Ti^{3+} species in TiO_2 can be totally balanced by oxygen vacancies, equal Ti^{3+} and oxygen vacancy should appear/disappear simultaneously; (2) besides Ti^{3+} and oxygen vacancy, a certain amount of structural defects (mainly refer to the local structural rearrangements in TiO_2) are present in the TiO_2 materials. This will lead to the inequalities between Ti^{3+} and oxygen vacancy in the material; (3) when the electric charges of Ti^{3+} species in TiO_2 are balanced by protons, Ti^{3+} has no direct connection with oxygen vacancy.

2.1 Partial reduction method

The partial reduction method starts from a Ti(IV)-containing precursor (including TiO_2), which is partially reduced by a suitable reductant under certain conditions to finally create a self-modified (or oxygen-deficient) TiO_2 materials. The specific means that were used in previously-reported partial reduction methods are summarized as below:
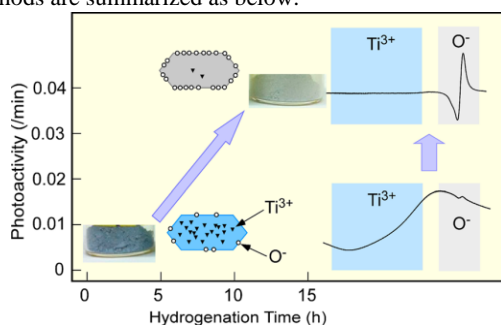
Fig. 1 Digital images and the electron paramagnetic resonance (EPR) spectra of H_2-treated TiO_2 samples with different reaction times.[22] Reprinted with permission from Ref. 22. Copyright 2013 American Chemical Society.

(i) High-Temperature Hydrogenation. Typically, TiO_2 samples are treated by H_2 at elevated temperatures to form self-modified TiO_2 materials.[21-26] During the hydrogenation process, H_2 will react with the lattice oxygen, leading to the formation of oxygen vacancies in TiO_2; and simultaneously one oxygen vacancy leave behind two excess electrons. These electrons can locate at titanium positions (*i.e.*, forming Ti^{3+}), and can also remain at the positions of oxygen vacancies (*i.e.*, forming electron-containing oxygen vacancies). It should be pointed out that the defect types are very sensitive to their formation

conditions, and different defect types might exist and coexist in the same sample. For example, H. Liu *et al.* showed that the H_2-treated samples obtained at < 450 ^{o}C possessed only single-electron-trapped oxygen vacancies (V_o), whereas the samples obtained at > 450 ^{o}C possessed both V_o˙ and Ti^{3+}.[21] In another example, X. Yu *et al.* showed that the defect types and their distribution between surface and bulk strongly depended on the hydrogenation temperature and time.[22] Longer hydrogenation at 600-700 ^{o}C induced the attenuation of Ti^{3+}, and the increase of O^- species (Fig. 1). The reason behind this phenomenon proposed by the authors is that bulk Ti^{3+} defects might diffuse to the surface and react with surface oxygen vacancies and absorbed oxygen molecules during longer hydrogenation, finally resulting into the formation of O^- species.

(ii) Reduction of Ti^{4+} by other reductants. In addition to H_2, other reductants, including metallic zinc, Al, diethylene glycol (DEG), $NaBH_4$ and CO, were also employed to produce self-modified TiO_2 materials.[27-32] Using the redox reaction between Zn and Ti^{4+} ($Zn + Ti^{4+} \rightarrow Zn^{2+} + Ti^{3+}$), Zheng *et al.* prepared stable Ti^{3+} self-doped TiO_2 with tunable phase composition.[27] In addition, Sayed and co-workers reported that TiO_2 was refluxed at 220 ^{o}C in DEG (a reducing agent and solvent) to form Ti^{3+}-contianing TiO_2 materials.[29] Kang *et al.* demonstrated that TiO_2 nanotube arrays were reduced by $NaBH_4$, a strong reducing agent.[30] The reaction was proposed as follows:

$$NaBH_4 + 8OH^- \rightarrow NaBO_2 + 8e^- + 6H_2O$$

$$Ti^{4+} + e^- \rightarrow Ti^{3+}$$
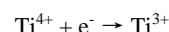
In another study, a combustion method was developed by Feng to synthesize self-modified TiO_2 materials using in situ generated reducing gases (CO and NO) as reductant. For instance, when a mixture containing ethanol, hydrochloric acid, titanium(IV) isopropoxide and ethylimidazole was introduced into a preheated oven (500 ~ 600 ^{o}C), bulk Ti^{3+} self-doped TiO_2 was directly obtained.[31] Using the similar combustion method, but replacing titanium(IV) isopropoxide with porous amorphous TiO_2, the same group successfully prepared stable titania material with a large number of V_o˙ defects (Fig. 2).[32]
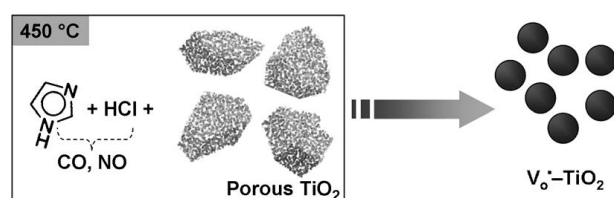
Fig. 2 Schematic representation for the synthesis of V_o˙-TiO_2 from porous amorphous TiO_2 in the presence of imidazole and HCl at 450 ^{o}C. The combustion of imidazole in the presence of HCl can release reducing gases, such as CO and NO.[32] Copyright 2013 WILEY-VCH Verlag GmbH & Co. KGaA Weinheim.

(iii) Hydro(solvo)thermal Synthesis. Hydro(solvo)thermal technique was reported to synthesize the self-modified TiO_2 materials by different groups.[33-34] Cheng group synthesized Ti^{3+}-doped anatase TiO_2 with {001} active facets by using TiB_2 as precursor in a HF-containing hydrothermal system (Fig. 3);[33] whereas Zhao group synthesized Ti^{3+}-doped anatase mesocrystals with {001} and {101} active facets by using titanium

isopropoxide as titanium source and formic acid as solvent.[34] Although the formation mechanism is still not clear in the above reaction systems, hydro(solvo)thermal technique has been proved to be very advantageous to combine defect engineering and facet control.
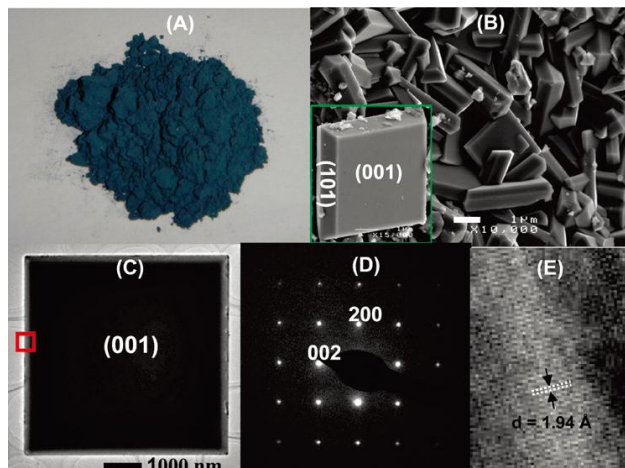
Fig. 3 Optical photo (A), typical SEM and TEM images (B and C), SAED patterns (D), and high-resolution TEM image (E) of oxygen deficient anatase TiO_2 sheets.[33] Reprinted with permission from Ref. 33. Copyright 2009 American Chemical Society.

(iv) Plasma Treatment, Vacuum Activation, and e-Beam Irradiation. In a low-temperature plasma, high-energy electrons and atoms are available to reduce the kin layer of TiO_2 materials, finally leading to the formation of self-modified TiO_2 materials.[35-38] This method has been employed by some Japanese researchers; and for example, TiO_2 materials with $V_o^{\cdot}$ defects were obtained by them.[35,36] By combining plasma and electrolysis, Zhang *et al.* synthesized oxygen-deficient TiO_2 microspheres that exhibited optical absorption covering the range from ultraviolet to infra-red.[37] In addition, vacuum treatment of TiO_2 at elevated temperatures can also produce oxygen-deficient TiO_2 materials, due to the release of lattice oxygen atoms under vacuum condition ($TiO_2 \rightarrow TiO_{2-x} + O_2$);[39] and e-beam irradiation method was reported to produce Ti^{3+}-TiO_2 because of the surface reduction by electrons.[40]

(v) Photochemical Synthesis. Photocatalysis phenomenon was discovered in 1972.[9] However, only in recent years photochemical technique was employed to synthesize the Ti^{3+} self-modified TiO_2 materials.[41-46] This is because 1) in common TiO_2 materials the amount of photogenerated Ti^{3+} species is rather limited; 2) the photogenerated Ti^{3+} was usually considered as an intermediate state in a photocatalytic system, and thereby its modification effects on the property of TiO_2 was often ignored. Up to now, there are three main types of TiO_2 materials that can be efficiently modified by photogenerated Ti^{3+}. They are porous amorphous TiO_2, TiO_2 gel, and amorphous TiO_2 nanoparticles. Let us take the porous amorphous TiO_2 material for an example.[41,42] This porous material possesses an ultra-large BET surface area of ~530 m^2/g. With UV irradiation, the color of the porous TiO_2 turned from white to intense blue under the protection of inert gas (Fig. 4A), which is indicative of the presence of a large number of Ti^{3+} species in the porous TiO_2. The presence of Ti^{3+} in the porous TiO_2 was confirmed by EPR

spectroscopy (Fig. 4B).[41] No paramagnetic signals were observed for porous amorphous TiO_2 before UV irradiation, whereas after UV-irradiation, an intense signal at g = 1.925 showed up. This EPR signal is ascribed to surface Ti^{3+}. In addition, the amount of photogenerated Ti^{3+} can be further increased by the introduction of dopant (*e.g.*, V^{4+}) in porous TiO_2.
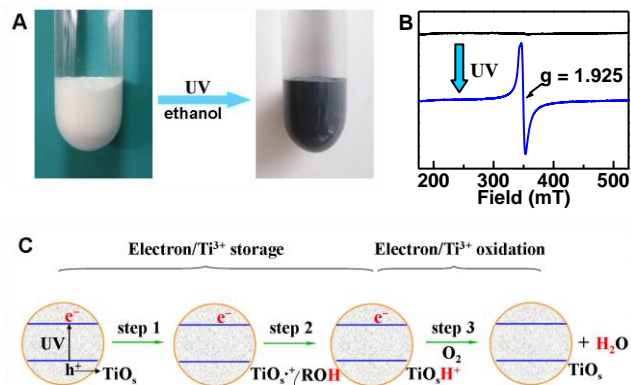
Fig. 4 Digital images (A) and EPR spectra (B) of porous amorphous TiO_2 before and after UV irradiation; (C) Schematic representation of photochemical synthesis (step 1 and step 2) of Ti^{3+}-containing TiO_2; and (step 3) oxidation of Ti^{3+} in TiO_2 by an oxidant, such as O_2. TiO_s and ROH denote the surface oxygen atom of TiO_2 and the hole scavenger, respectively. In this scheme, photogenerated electrons are present in the form of Ti^{3+}, and Ti^{3+} storage and oxidation are proton-coupled processes.[41] Reproduced by permission of The Royal Society of Chemistry.

The photogenerated Ti^{3+} in TiO_2 is fundamentally different from those formed through other routes. The differences mainly include: 1) The photogenerated Ti^{3+} ions only exists on the TiO_2 surface; 2) they are sensitive to the oxidants, such as O_2; 3) their electric charges are balanced by the surface protons, rather than the oxygen vacancies; and 4) their generation and consumption are proton-coupled processes. Because of these differences, the photochemically-synthesized Ti^{3+}-TiO_2 showed many unique properties and functions (see below).

Fig. 4C shows schematic representation of photochemical synthesis (step 1 and step 2) of Ti^{3+}-TiO_2; and (step 3) oxidation of Ti^{3+} in TiO_2 by an oxidant, such as O_2. When an incident light possessing energy greater than band gap of TiO_2 (*i.e.*, UV light) hits the material, electrons in the valence band are excited to the conduction band, concomitantly leaving holes in the valance band. The photo-generated electrons and holes will allow reduction and oxidation reactions, respectively, to occur on the TiO_2 surface. In a typical photochemical system for the synthesis of Ti^{3+}-TiO_2, a proper hole scavenger (*e.g.*, ethanol) but no electron scavenger are needed in the reaction system. In this case, the photogenerated holes on the valence band react with the hole scavenger, and the electrons are comfortably stored in the form of Ti^{3+} (step 1 and 2). When the photogenerated Ti^{3+} contacts with a proper oxidant, such as O_2, it will be consumed rapidly (step 3). It should be emphasized that the Ti^{3+} storage and oxidation are proton-coupled processes.

2.2 Partial oxidation method

Although the +4 oxidation state dominates titanium chemistry, compounds in the +2 and +3 oxidation states are also common.

The Ti-based compounds with low oxidation states include TiH_2, TiO, Ti_2O_3, $TiCl_3$. Considering that it is possible to obtain Ti^{3+} self-doped TiO_2 materials by partial oxidation of these compounds under an appropriate condition, researchers have been exploring synthetic approaches for translating this idea into reality.[47-51]
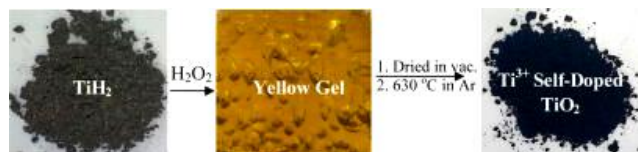
Fig. 5 Scheme of the synthesis of Ti^{3+}-TiO_2 form TiH_2. Gray TiH_2 powder was first converted to yellowish gel after reaction with H_2O_2. The gel was further heated to yield the black Ti^{3+}-TiO_2 powder at high temperatures.[47] Reprinted with permission from Ref. 47. Copyright 2013 American Chemical Society.

Recently, Grabstanowicz *et al.* reported the synthesis of Ti^{3+} self-doped rutile TiO_2 using TiH_2 as precursor.[47] As shown in Fig. 5, they first used 30% aqueous solution of H_2O_2 to oxidize gray TiH_2 powders, yielding a yellow or green gel-like product.[47] The selection of H_2O_2 as the oxidation agent is because 1) TiH_2 is stable in air and water, but very reactive with H_2O_2 at room temperature; 2) the only byproduct of H_2O_2 is H_2O, avoiding any unnecessary contaminations. Finally, the dried gel was thermally treated at 630 ^{o}C in Ar to form Ti^{3+} self-doped rutile TiO_2 material. Furthermore, Liu *et al.* showed that rice-shaped Ti^{3+} self-doped anatase nanoparticles were synthesized by direct hydrothermal treatment of TiH_2 in H_2O_2 aqueous solution (Fig. 6).[48] From the above results, it is concluded that even using the same precursor (*i.e.*, TiH_2) and oxidation agent (H_2O_2), different thermal treatment methods can lead to different products (*e.g.*, *rutile* phase obtained in the former method, but *anatase* phase obtained in the later method).
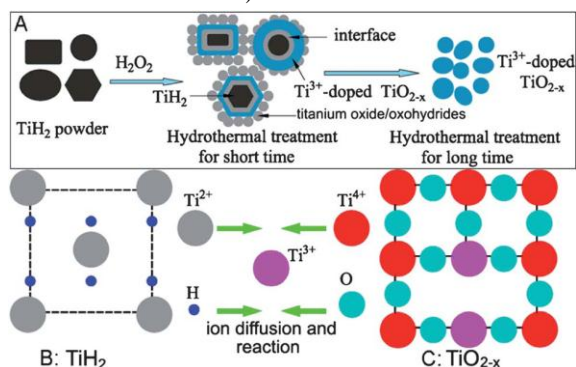
Fig. 6 (A) Schematic of the formation mechanisms for the Ti^{3+} self-doped nantase TiO_2 nanoparticles; and (B, C) the interface diffusion–redox diagram. The green arrows indicate ion diffusion.[48] Reproduced by permission of The Royal Society of Chemistry.

In addition to TiH_2, TiO, Ti_2O_3 and Ti were also proved to be efficient precursors for the synthesis of self-modified TiO_2 materials.[49-51] Pei *et al.* demonstrated the synthesis of a self-doped TiO_2 material with Ti^{3+} and $V_o^{\cdot}$ defects by hydrothermal treatment of TiO in HCl solution.[49] They claimed that in the present reaction system, Ti^{3+} species can be generated via the reaction between TiO and HCl (TiO + HCl → Ti^{3+} +H_2 +H_2O). Liu *et al.* showed that direct thermal oxidation of Ti_2O_3 and TiO

mixture in air at 900 ^{o}C could also produce the Ti^{3+} self-doped TiO_2 mateial.[50] In another study, Zuo et al. synthesized Ti^{3+}-doped rutile TiO_2 with {110} active facets by using titanium powder as precursor in a HCl-containing hydrothermal system.[51]
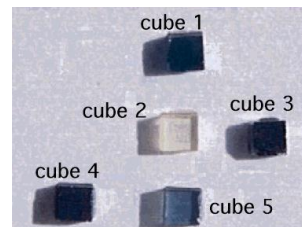
Fig. 7 Digital images of five rutile crystals with increased amount of bulk defects in the order of cube 2 < cube 5< cube 1 < cube 4 < cube 3. The lighter crystal possesses a lower amount of bulk defects.[52] Reprinted with permission from Ref. 52. Copyright 2001 American Chemical Society.

Table 1. Sample Resistivity (Ω/cm)[52]

	cube 2	cube 5	cube 1	cube 4	cube 3
resistivity	1835.0	108.24	46.76	24.06	8.94

3. Properties and functions of self-modified TiO_2

Defects in TiO_2 have often been considered to have negative influences on the properties of materials only. For example, the structural defects in TiO_2 were frequently referred by researchers to function as combination sites of photogenerated changes that lead to a low photocatalytic activity. However, recent studies show that proper defects can improve the properties of materials in some cases, and even result into some new useful functionalities that are not available to the "perfect" material, in the other cases. Herein we specially summarized the favorable effects of these defects on materials' properties and applications (see below).

3.1 Conductivity

In 2000, Diebold group investigated the influence of the Ti^{3+}-related bulk defects on the properties of TiO_2(110) single crystals.[52] In their study, TiO_2(110) cubes were cut from the same crystal and were heated in ultrahigh vacuum to produce the Ti^{3+}-related bulk defects in TiO_2. As shown in Fig. 7, five rutile crystals with different colors were prepared. The lighter crystal possessed a lower amount of bulk defects, and the amount of bulk defects increased in order of cube 2 < cube 5< cube 1 < cube 4 < cube 3. Table 1 shows the resistivity of the five cubes at 300 K. The results show that the darker crystal with a larger amount of defects has a lower resistivity than the lighter crystal with a smaller amount of defects. For example, the resistivity of cube 2 (the lightest one) is 1835.0 Ω/cm, whereas the resistivity of cube 3 (the darkest one) is only 8.94 Ω/cm. The resistivity of the former is about 205 times as high as that the latter. In another study, Chen group reported a porous crystalline titania material with heavily self-doped Ti^{3+} species in 2013.[53] In the material obtained, 29% of the titanium species in TiO_2 are present in the form of Ti^{3+}, so this material is heavily self-doped by Ti^{3+}. They further measured the room-temperature electrical conductivity, and the result showed that the material exhibited a conductivity of 2.7×10^{-3} S/cm whereas the conductivity value of Ti^{3+}-free sample was 9.7×10^{-8} S/cm. In other words, the conductivity of Ti^{3+}-TiO_2 increased by ~5 orders of magnitude in comparison

with that of Ti^{3+}-free TiO_2 sample. The increase in conductivity (or the decrease in resistivity) of TiO_2 by Ti^{3+} self-modification was considered to be because Ti^{3+} species in TiO_2 can function as efficient donors, the electrons of which could hop to the conduction band (or adjacent Ti^{4+} sites).[53-57]

3.2 Magnetism

Dilute magnetic semiconductors (DMS), in particular the ferromagnetic oxides, have received great attention because of their potential applications in spintronics.[58] The study of DMS was significantly accelerated by the discovery of room-temperature ferromagnetism in Co-doped TiO_2 film.[58] With the development of DMS studies, the researchers surprisingly found that some defect-containing undoped TiO_2 materials (without introducing magnetic ions in the materials) also exhibited room-temperature ferromagnetism although TiO_2 itself is intrinsically non-magnetic.

In 2006, Yoon et al. observed that oxygen-deficient anatase TiO_2 film showed high-temperature ferromagnetism with a Curie temperature up to 880 K.[59] In this study, the oxygen defects were found to locate at the interface between the anatase TiO_2 film and the (100) oriented lanthanum aluminate ($LaAlO_3$) substrates because of the presence of atomic mismatch at the interface. The authors also showed that the interfacial oxygen defects in the anatase TiO_2 film on a (100) $LaAlO_3$ substrate are the origin of the observed magnetism. Furthermore, the authors proposed that the oxygen vacancy-related Ti^{3+} and Ti^{2+} species might provide the magnetic moments because of their $3d^1$ and $3d^2$ electronic configurations, respectively, although no evidences were provided to support the presence of Ti^{3+} and Ti^{2+} in the material. However, in a theoretical study by Kim et al., the ferromagnetism in undoped TiO_2 was thought be the result of the charge redistribution owing to the oxygen-vacancy-induced lattice distortion.[60]
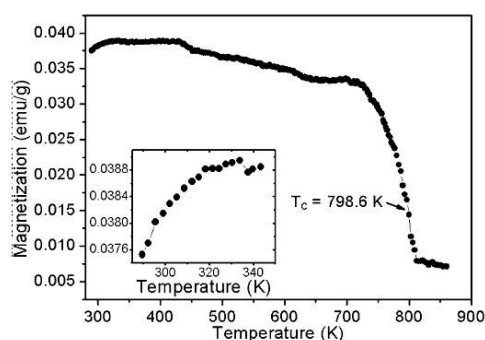
Fig. 8 Temperature dependent magnetization (M–T) curve of oxygen-deficient TiO_2 nanobelts showing a ferromagnetic to paramagnetic transition at ~800 K.[62] Reproduced by permission of The Royal Society of Chemistry.

More recently, several different groups experimentally showed Ti^{3+} ions with one unpaired 3d electron ($3d^1$) provided the local magnetic moments in the undoped TiO_2 materials. Zhou group prepared Ti^{3+} self-doped rutile TiO_2 single crystal by oxygen ion irradiation method, and observed ferromagnetism in the obtained material.[61] In addition, Chen group prepared porous amorphous TiO_2 with a large number of Ti^{3+} by a photochemical method.[41] The investigation in magnetic properties of the Ti^{3+}-TiO_2

revealed the co-existence of ferromagnetism and paramagnetism in the material. When the Ti^{3+} in TiO_2 was completely consumed by air, the as-obtained Ti^{3+}-free TiO_2 turned diamagnetic. This observation strongly confirmed that the magnetism of the Ti^{3+}-TiO_2 was an intrinsic feature associated with the Ti^{3+} species. Furthermore, Santara and co-workers reported on the oxygen vacancy induced ferromagnetism above room temperature in undoped TiO_2 nanoporous nanoribbons (Fig. 8).[62] The observed magnetism was explained by the s-d interaction between the $1s^1$ electron spin in $V_o^{.}$ and the $3d^1$ electron spin of Ti^{3+} ions. However, it should be noted that the exact mechanism of the magnetism for undoped TiO_2 is still not very clear at current stage. Thus, further experimental and theoretical studies on this unusual magnetic phenomenon should be strongly encouraged.

3.3 Sensing application

TiO_2, a wide band gap semiconductor, is a well-established oxide material that has been employed as a promising candidate in sensing applications. Previously, surface modification with noble metal particles or other metal oxides was often attempted to improve the sensing properties of TiO_2.[3] Recently, Chen group showed the importance of Ti^{3+} defects in TiO_2-based sensors for the first time, providing a new strategy to optimize TiO_2 sensing properties. In their study, thermally stable, Ti^{3+} self-modified TiO_2 nanomaterials were demonstrated to exhibit enhanced sensitivity and ultrafast response/recovery (< 3 s) for the detection of various organic vapors, such as ethanol, methanol and acetone.[63] The enhanced gas-sensing performances for Ti^{3+} self-modified TiO_2 materials could be related to the Ti^{3+}-induced enhancement of oxygen absorption on TiO_2 surfaces. Because the Ti^{3+} species in these nanomaterials were deeply buried in the bulk of the TiO_2 particles, the Ti^{3+} effect on increasing the surface reaction activity of TiO_2 is limited. This thereby led to a high operating temperature (300 °C) that was needed for sensing application. In view of this, the same group reported another porous crystalline titania with heavily self-doped Ti^{3+} species.[53] This Ti^{3+} self-doped TiO_2 material contained a considerable proportion of Ti^{3+} in the subsurface region of the titania particles, and thus served as an efficient room-temperature gas-sensing material for specific CO detection with fast response/recovery. The self-dopant (Ti^{3+}) in the titania material proved to possess dual functions: (1) decreasing the resistance of TiO_2 significantly; and (2) increasing the chemisorbed oxygen species substantially.
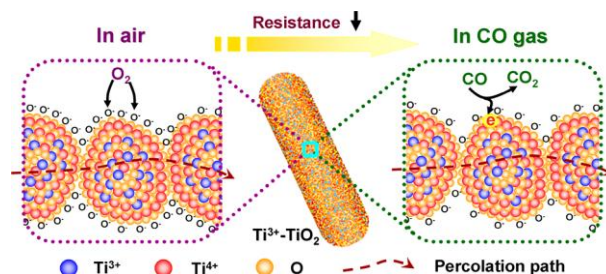
Fig. 9 Schematic representation of the sensing mechanism of Ti^{3+}-containing TiO_2. Resistance ↓ means resistance decrease. Percolation path means electron transport pathway between the Au electrodes of the sensor.[53] Reprinted with permission from Ref. 53. Copyright 2013 American Chemical Society.

As shown in Fig. 9, the sensing mechanism of Ti^{3+} self-doped

TiO_2 was discussed by Chen *et al*,[53] based on the interaction of surface chemisorbed oxygen and the CO gas at room temperature. When the TiO_2 sensor is exposed to air, the oxygen molecules in air are chemisorbed on the TiO_2 surface and then extract electrons from the TiO_2. This will result in a potential barrier and thus a high-resistance state. On the other hand, when the sensor is exposed to CO gas, the latter reacts with the surface oxygen species, reducing the amount of surface adsorbed oxygen. This finally leads to a decreased potential barrier and thus a low-resistance state. For such a surface reaction, the increase in amount of surface-adsorbed oxygen should be beneficial to the reaction activity/kinetics for oxidation of the CO gas on the TiO_2 surface. In addition, the decrease in electrical resistance not only makes it feasible to detect the resistance (and its variation) for a room-temperature sensor but also enables the rapid electron transport between the Au electrodes of the sensor. Therefore, the simultaneous accomplishment of high oxygen adsorption and low electrical resistance by the Ti^{3+} self-doping played a crucial role in the room-temperature sensing performance of the Ti^{3+}-TiO_2 material.

In another study, Pan *et al.* showed that Ti^{3+} self-doped rutile was used for direct and ultrafast detection of H_2O_2.[64] This detection was based on the fast color change from blue to yellow when Ti^{3+} self-doped rutile was exposed to H_2O_2. The proposed chemical mechanism was shown by the equation:

$$Ti^{3+} \text{ (blue)} + H_2O_2 + 2H_2O \rightarrow H_2TiO_4 \text{ (yellow)} + 3H^+$$
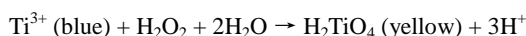
3.4 Photocatalytic hydrogen evolution and degradation of organic compounds

In 1972, Fujishima and Honda discovered the photoinduced water splitting on TiO_2 electrodes.[9] Since then, photocatalytic H_2 production over TiO_2 materials is long considered as a promising approach for solar energy exploitation, especially because H_2 is attractive as a clean fuel. However, the widespread use of TiO_2 material is limited by its wide band-gap energy, which causes the catalyst to exploit only a very small proportion (about 3–5%) of solar radiation. Recently, self-modification strategy was demonstrated to be one of effective methods to shift the photo-responsive range of TiO_2 to visible spectral region.
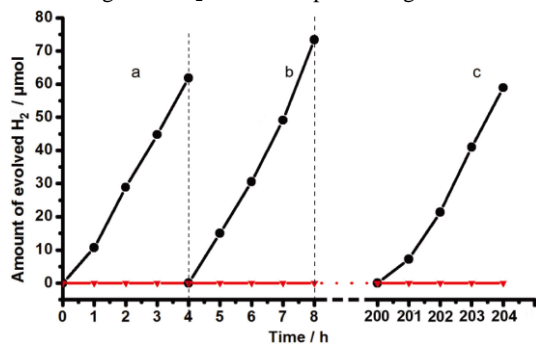
Fig. 10 Time courses of evolved H_2 under visible light (> 400 nm) illumination over Ti^{3+} self-doped TiO_2 synthesized from a combustion method.[31] Reprinted with permission from Ref. 31. Copyright 2010 American Chemical Society.

The first attempt at visible-light-driven photocatalytic H_2 evolution over self-modified TiO_2 was reported by Feng group.[31] Through a facile combustion method, Feng *et al.* prepared Ti^{3+} self-doped TiO_2, which possessed high stability in air or water

under irradiation, and visible-light activity for H_2 evolution from a methanol-water mixture (Fig. 10). Because the combustion process was very harsh, this method only yielded the irregularly shaped products. To overcome this shortcoming of combustion method, the same group developed a hydrothermal method to grow Ti^{3+} self-doped rutile TiO_2 crystals with highly active facets.[51] This material showed enhanced photocatalytic activity relative to the irregular nanoparticles prepared by a combustion method, which was attributed to the exposure of active {110} facets on the material. In another study, this group also reported a dopant-free, visible-light-responsive TiO_2 photocatalyst with $V_o^·$ defects. This material exhibited not only satisfactory thermal and photo-stability, but also superior photocatalytic activity for H_2 evolution (115 μmol/h/g) from water with methanol as sacrificial reagent under visible light ($\lambda > 400$ nm) irradiation.[32] After Feng's pioneering work, there were several reports on new methods to synthesize the self-modified TiO_2 materials (*e.g.*, vacuum activity, and selective oxidation TiH_2 or TiO) and their visible light activity for H_2 evolution.[28,39,48,49,65]

In addition to photocatalytic H_2 evolution, photocatalytic degradation of organic compounds by self-modified TiO_2 materials were also reported for potential environmental remediation using visible light.[21,22,25,27,28,38,39,47,48,50,65,66] In these studies, a range of organic compounds, including benzoic acid, 2-propanol, methylene blue (MA) and methyl orange (MO), were decomposed into CO_2 and H_2O under visible light. For example, Liu *et al.* demonstrated that the Ti^{3+} self-doped TiO_2 becomes an efficient visible light active photocatalyst for degradation of 2-propanol by the grafting of Cu(II) oxide amorphous nanoclusters.[50] The results showed that the presence of Ti^{3+} nearly did not narrow the band gap, but led to the formation of isolated states between the forbidden gap. These isolated states have various electric levels from 0.3 to 0.8 eV below the conduction band minimum, resulting into the broad visible light absorption in the Ti^{3+} self-doped TiO_2 materials. On the other hand, the Cu(II) oxide nanoclusters functioned as a co-catalysts to suppress the recombination of photogenerated charges.

3.5 Other photocatalytic reactions

Zhao and co-workers studied the photocatalytic reduction and oxidation of nitrosobenzene over Ti^{3+} self-doped TiO_2 mesocrystals.[34] They found that the synergetic effect between Ti^{3+} and the (101)/(001) facet ratio are responsible for the higher activity of the TiO_2 mesocrystals for both oxidation and reduction of nitrosobenzene. The authors claimed that the (101) facet was intrinsically more active than (001) facet, and the existence of Ti^{3+} defects could shift the valence band maximum downwards and facilitated the generation of strongly reductive electrons. Note that in their study no visible-light photocatalytic activity was observed.

However, in another study Mul *et al.* showed that Ti^{3+} self-doped titania with a bandgap of 2.93 eV served as a photocatalyst for the liquid phase selective oxidation of methylcyclohexane under both UV and visible light irradiation.[67] The activity of Ti^{3+} self-doped titania surpassed those of the commercial titania catalysts, such as TiO_2 P25. In addition, Nakamura *et al.* demonstrated that self-modified TiO_2 with $V_o^·$ defects possessed the photocatalytic activity for NO oxidation in the visible light region up to 600 nm.[35,36] The oxidation of NO under visible light

proceeded consecutively as $NO \rightarrow NO_2^- \rightarrow NO_3^-$. The visible light activity of V_o·-modified TiO_2 was attributed to the presence of oxygen vacancy state between the valence and the conduction bands in the TiO_2 band structure.

3.6 Photoelectrochemical water splitting

In 2011, Li and co-workers demonstrated for the first time that hydrogen treatment on TiO_2 nanowires and nanotubes created a high density of oxygen vacancies, and thus significantly improved the performance of TiO_2 materials for photoelectrochemical water splitting (Fig. 11).[26] In comparison to pristine TiO_2 nanowires, the TiO_2 samples after hydrogen treatment showed obviously enhanced photocurrent in the entire potential window, and low photocurrent saturation potentials of -0.6 V vs Ag/AgCl (0.4 V vs RHE). The optimized TiO_2 nanowire sample gave a photocurrent density of ~1.97 mA/cm^2 at -0.6 V vs Ag/AgCl under the illumination of simulated solar light (100 mW/cm^2 from 150 W xenon lamp), and a solar-to-hydrogen efficiency was calculated to be around 1.1%. Furthermore, the incident-photon-to-current-conversion efficiency (IPCE) spectra showed the photocurrent enhancement by hydrogen treatment was mainly due to the improved photoactivity of TiO_2 in the UV region (Fig. 11).
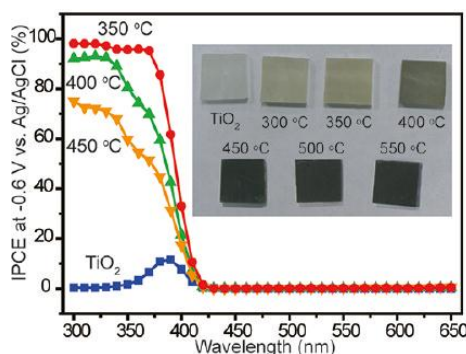
Fig. 11 IPCE spectra of pristine TiO_2 and several TiO_2 nanowires prepared by hydrogen treatment at 350, 400, and 450 °C.[26] Reprinted with permission from Ref. 26. Copyright 2011 American Chemical Society.

To enhance the visible light water splitting performance of TiO_2 nanowires, C. B. Mullins and the coworkers showed hydrogenation and nitridation cotreatment of TiO_2 nanowires as a simple and effective method. This cotreatment led to the codoping of nitrogen and Ti^{3+} in TiO_2 nanowires.[23] The synergistic effect between the N-dopant and Ti^{3+} was believed to be the key to the extension of the active spectrum and the superior visible light water splitting activity. In other studies,[30,68] Ti^{3+} self-doped TiO_2 nanotubes were prepared by either chemical reduction or electrochemical reduction, and they all exhibited enhanced water splitting performances, regardless of the methods they used.

3.7 Proton-coupled electron transfer agents

Although it is well-known that Ti^{3+} self-modified TiO_2 materials (Ti^{3+}-TiO_2) can be synthesized by a photochemical method (as mentioned before), it is little-known that the Ti^{3+}-TiO_2 materials obtained by such a method can serve as proton-coupled electron transfer agents. In 2010, Zou *et al.* developed a photochemical approach for the preparation of porous TiO_2 with

a large number of Ti^{3+} species.[41] When studying the interaction of Ti^{3+} in TiO_2 with nitrobenzene, they found that the TiO_2 with Ti^{3+} species supplied not only electrons (*i.e.*, Ti^{3+}) but also protons (H^+) for the transformation of nitrobenzene into aniline. They realized that when an electron (in Ti^{3+}) was released to an electron acceptor such as nitrobenzene, a proton (H^+) on the surface of the TiO_2 was also removed at the same time. However, in their paper,[41] the concept "proton-coupled electron transfer (PCET)" was not proposed. In 2012, Schrauben *et al.* showed that photochemically reduced (or Ti^{3+} self-modified) TiO_2 nanoparticles in solution transferred an electron and a proton to phenoxyl and nitroxyl radicals, indicating that e$^-$ and H^+ were coupled in this interfacial reaction.[44] The concept of PCET was suggested by the authors, and correspondingly the Ti^{3+}-TiO_2 materials synthesized by a photochemical method could serve as proton-coupled electron transfer agents. The above observations had important implications for the understanding and development of chemical energy technologies, such as photocatalysis, that were usually previously considered as electron transfer process, rather than proton-coupled electron transfer process.

In a recent study, Su *et al.* reported a vanadium-doped porous TiO_2 with highly active hydrogen (V–$TiO_2(H^*)$) prepared by a photochemical method.[42] The vanadium-doping could increase the amount of active hydrogen in the obtained TiO_2 material. The active hydrogen (H^*) in this material is not molecular hydrogen but a proton with an electron (*i.e.*, Ti^{3+}) in its vicinity. Furthermore, the authors used the as-obtained TiO_2 materials as proton-coupled electron transfer agents for the chemoselective hydrogenation of nitroarenes. The results showed that the TiO_2 materials can instantly (< 10 s) and selectively reduce nitroarenes to aminoarenes under ambient conditions. During the reduction process, the V–$TiO_2(H^*)$ provided rich H^* species (*i.e.*, coupled e$^-$ and H^+), which could be regenerated through UV light irradiation of the reactant in methanol after the consumption of the H^* species (Fig. 12).
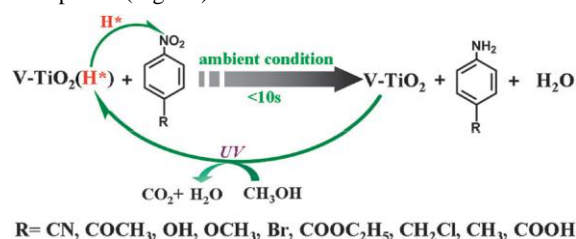
Fig. 12 Schematic diagram for selective hydrogenation of nitroarenes to aminoarenes by V–$TiO_2(H^*)$ and the regeneration process of V–$TiO_2(H^*)$. The active hydrogen (H^*) in our material is not molecular hydrogen but a proton with an electron in its vicinity.[42] Reproduced by permission of The Royal Society of Chemistry.

4. Conclusions

In this article, we reviewed recent development in the synthesis of self-modified TiO_2 materials with Ti^{3+} ions and/or oxygen vacancies, and some favorable effects of these defects on properties and applications of materials. Despite the enormous strides and many achievements made in the field of TiO_2 defect chemistry, as outlined in this review, there are still a lot of intractable difficulties ahead, such as the identification of nature

and local microstructure of Ti^{3+}/oxygen defects. In addition, exploring new applications related to Ti^{3+}/oxygen defects and understanding the functions of these defects still remain challenging. This, therefore, calls for more research efforts in general defect chemistry of metal oxides—a burgeoning and fascinating area of chemistry.

Acknowledgements

Notes and references

^{a} School of Chemistry and Chemical Engineering, Shanghai Jiao Tong University, Shanghai 200240, China. E-mail: chemcj@sjtu.edu.cn

^{b} State Key Lab of Inorganic Synthesis & Preparative Chemistry, College of Chemistry, Jilin University, Changchun 130012, China. E-mail: chemistryzouxx@gmail.com

1   O. Carp, C. L. Huisman and A. Reller, *Prog. Solid State Chem.*, 2004, **32**, 33.
2   H. Chen, C. E. Nanayakkara and V. H. Grassian, *Chem. Rev.*, 2012, **112**, 5919.
3   X. Chen and S. S. Mao, *Chem. Rev.*, 2007, **107**, 2891.
4   T. L.Thompson and J. T. Yates, Jr., *Chem. Rev.*, 2006, **106**, 4428.
5   A. L. Linsebigler, G. Lu and J. T. Yates, Jr., *Chem. Rev.,* 1995, **95**, 735.
6   S. G. Kumar and L. G. Devi, *J. Phys. Chem. A*, 2011, **115**, 13211.
7   T. Tachikawa, M. Fujitsuka and T. Majima, *J. Phys. Chem. C*, 2007, **111**, 5259.
8   M. Ni, M. K.H. Leung, D. Y. C. Leung and K. Sumathy, *Renewable Sustainable Energy Rev.*, 2007, **11**, 401.
9   A. Fujishima and K. Honda, *Nature*, 1972, **238**, 37.
10 C. D. Valentin, G. Pacchioni and A. Selloni, *J. Phys. Chem. C*, 2009, **113**, 20543; X.-X. Zou, G.-D. Li, J. Zhao, J. Su, X. Wei, K.-X. Wang, Y.-N. Wang and J.-S. Chen, *Int. J. Photoenergy.*, doi:10.1155/2012/720183; C. H. Chen, T. C. Chen, C. C. Chen, Y. T. Lai, J. H. You, T. M. Chou, C. H. Chen and J. F. Lee, *Langmiur*, 2012, **28**, 9996; K. Suriye, P. Praserthdam and B. Jongsomjit, *Ind. Eng. Chem. Res.*, 2005, **44**, 6599; L. B. Xiong, J. L. Li, B. Yang and Y. Yu, *J. Nanomater.*, 2012, DOI: 10.1155/2012/831524; Y. B. He, O. Dulub, H. Z. Cheng, A.Sellini and U. Diebold, *Phys. Rev. Lett.*, 2009, **102**, 106105; M. Aizawa, Y. Morikawa, Y. Namai, H. Morikawa and Y. Iwasawa, *J. Phys. Chem. B*,2005, **109**, 18831.
11 J. Chen, L. B. Lin and F. Q. Jing, *J. Phys. Chem. Solids.*, 2001, **62**, 1257; E. Finazzi, C. D. Valentin, G. Pacchioni and A. Selloni, *J. Chem. Phys.*, 2008, **129**, 154113; J. Zhao, X. X. Zou, J. Su, P. P. Wang, L. J. Zhou and G. D. Li, *Dalton Trans.*, 2013, **42**, 4365; N. A. Deskins, R. Rousseau and M. Dupuis, *J. Phys. Chem. C.*, 2011, **115**, 7562; Z. Lin, A. Orlov, R. M. Lambert and M. C. Payne, *J. Phys. Chem. B*, 2005, **109**, 20948; X. Zou, Z. Tao and T. Asefa, *Curr. Org. Chem.*, 2013, **17**, 1274; E. Lira, S. Wendt, P. Huo, J. Hansen, R. Streber, S. Porsgaard, Y. Y. Wei, R.Bechstein, E. Lægsgaad and Besenbacher, *J. Am. Chem. Soc.*, 2011, **133**, 6529; N. G. Petrik, Z. Zhang, Y. Du, Z. Dohnálek, I. Lyubinetsky and G. A. Kimmel, *J. Phys. Chem. C*, 2009, **113**, 12407; R. Schaub, E. Wahlström, A. Rønnau, E. Lægsgaard, I. Stensgaard, I. Stensgaard, F. Besenbacher, *Science*, 2003, **299**, 377; M. Setvin, U. Aschauer, P. Scheiber, Y. F. Li, W. Hou, M. Schmid, A. Selloni and U. Diebold, *Science*, 2013, **341**,988; S. Livraghi, S. Maurelli, M. C. Paganini, M. Chiesa and E. Giamello, *Angew.Chem. Int. Ed.*, 2011, **50**, 8038.
12 R. Asahi, T. Morikawa, T. Ohwaki, K. Aoki and Y. Taga, *Science*, 2001, **293**, 269.
13 D. V. Bavykin, J. M. Friedrich, and F. C. Walsh, *Adv. Mater.*, 2006, **18**, 2807.
14 S. In, A. Orlov, R. Berg, F. Garcáa, S. Pedrosa-Jimenez, M. S. Tikhov, D. S. Wright and R. M. Lambert, *J. Am. Chem. Soc.*, 2007, **129**, 13790.
15 R. Niishiro, R. Konta, H. Kato, W.-J Chun, K. Asakura and A. Kudo, *J. Phys. Chem. C*, 2007, **111**, 17420.
16 J. Su, X. Zou, G.-D. Li, Y.-M. Jiang, Y. Cao, J. Zhao and J.-S. Chen, *Chem. Commun.*, 2013, **49**, 8217; X.-X. Zou, G.-D. Li, M.-Y. Guo, X.-H. Li, D.-P. Liu, J. Su, J.-S. Chen, *Chem. Eur. J.*, 2008, **14**, 11123.
17 A. Testino, I. R. Bellobono, V. Buscaglia, C. Canevali, M. D'Arienzo, S. Polizzi, R. Scotti and F. Morazzoni, *J. Am. Chem. Soc.*, 2007, **129**, 3564.
18 J. Pan, G. Liu, G. Q. Lu and H. M. Cheng, *Angew. Chem., Int. Ed.*, 2011, **50**, 2133.
19 H. G. Yang, C. H. Sun, S. Z. Qiao, J. Zou, G. Liu, S. C. Smith, H. M. Cheng and G. Q. Lu, *Nature*, 2008, **453**, 638.
20 X. Zou, R. Silva, X. Huang, J. F. Al-Sharab and T. Asefa, *Chem. Commun.*, 2013, **49**, 382.
21 H.Liu, H. T. Ma, X. Z. Li, M. Wu and X. H. Bao, *Chemosphere*, 2003, **50**, 39.
22 X. Yu, B. Kim and Y. K. Kim, *ACS Catal.*, 2013, **3**, 2479.
23 S. Hoang, S. P. Berglund, N. T. Hahn, A. J. Bard and C. B. Mullins, *J. Am. Chem. Soc.*, 2012, **134**, 3659.
24 A. Naldoni, M. Allieta, S. Santangelo, M. Marelli, F. Fabbri, S. Cappelli, C. L. Bianchi, R. Psaro and V. D. Santo, *J. Am. Chem. Soc.*, 2012, **134**, 3659.
25 W. Wang, C. Lu, Y. Ni, M. Su and Z. Xu, *Appl. Catal. B Environ.*, 2012, **127**, 28.
26 G. Wang, H. Wang, Y. Ling, Y. Tang, X. Yang, R. C. Fitzmorris, C. Wang, J. Z. Zhang and Y. Li, *Nano lett.*, 2011, **11**, 3026.
27 Z. Zheng, B. Huang, X. Meng, J. Wang, S. Wang, Z. Lou, Z. Wang, X. Qin, X. Zhang and Y. Dai, *Chem. Comm.*, 2013, **49**, 868.
28 C. Yang, Z. Wang, T. Lin, H. Yin, X. Lu, D. Wang, T. Xu, C. Zheng, J. Lin, F. Huang, X. Xie and M. Jiang. *J. Am. Chem.Soc.*, 2013, **135**, 17831.
29 F. N. Sayed, O. D. Jayakumar, R. M. Kadam, S. R. Bharadwaj, L. Kienle, U. Schürmann, S. Kaps, R. Adelung, J. P. Mittal and A. K. Tyagi, *J. Phys. Chem. C*, 2012, **116**, 12462.
30 Q. Kang, J. Cao, Y. Zhang, L. Liu, H. Xu and J. Ye, *J. Mater. Chem. A*, 2013, **1**,5677.
31 F. Zuo, L. Wang, T. Wu, Z. Zhang, D. Borchardt, P. Feng, *J. Am. Chem. Soc.*, 2010, **132**, 11856.
32 X. Zou, J. Liu, J. Su, F. Zuo, J. Chen and P. Feng, *Chem. Eur. J.*, 2013, **19**, 2866.
33 G. Liu, H. G. Yang, X. Wang, L. Cheng, H. Lu, L. Wang, G. Q. Lu and H.-M. Cheng, *J. Phys. Chem. C*, 2009, **113**, 21784.
34 Q. Chen, W. Ma, C. Chen, H. Ji, J. Zhao, *Chem. Eur. J.*, 2012, **18**, 12584.
35 I. Nalamura, N. Negishi, S. Kutsuna, T. Ihara, S. Sugihara, K. Takeuchi, *J. Mol. Catal. A: Chem.*, 2000, **161**, 205.
36 I. Nakamura, S. Sugihara, K. Takeuchi, *Chem. Lett.*, 2000, **1**, 1276.
37 Z. K. Zhang, M. L.Bai, D. Z. Guo, S. M. Hou and G. M. Zhang, *Chem. Commun.*, 2011, **47**, 8439.
38 T. Ihara, M. Miyoshi, *J. Mater. Sci.*, 2001, **36**, 4201.
39 M. Xing, J. Zhang, F. Chen and B. Tian, *Chem. Commun.*, 2011, **47**, 4947.
40 S. Kim, W. J. Jo, D. Lee, S. H. Baeck, J. H. Shin and B. C. Lee, *Bull. Korean Chem. Soc.*, 2013, **34**, 5.
41 X.-X. Zou, G.-D. Li, K.-X. Wang, L. Li, J. Su and J.-S. Chen, *Chem. Comm.*, 2010, **46**, 2112.
42 J. Su, X.-X. Zou, G.-D. Li, L. Li, J. Zhao and J.-S. Chen, *Chem. Comm.*, 2012, **48**, 9032.
43 X.-X. Zou, G.-D. Li, Y.-N. Wang, J. Zhao, C. Yan, M.-L. Guo, L. Li and J.-S. Chen, *Chem. Comm.*, 2011, **47**, 1066.
44 J. N. Schrauben, R. Hayoun, C. N. Valdez, M. Braten, L. Fradley and J. M. Mayer, *Science*, 2012, **336**, 1289.
45 A. I. Kuznetsov, O. Kameneva, A. Alexandrov, N. Bityurin, K. Chhor and A. Kanaev, *J. Phys. Chem. B*, 2006, **110**, 435.
46 A. I. Kuznetsov, O. Kameneva, L. Rozes, C. Sanchez, N. Bityurin and A. Kanaev, *Chem. Phys. Lett.*, 2006, **429**, 523.
47 L. R. Grabstanowicz, S. Gao, T. Li, R. M. Rickard, T. Rajh, D.-J. Liu and T. Xu, *Inorg. Chem.*, 2013, **52**, 3884.

48 X. Liu, S. Gao, H. Xu, Z. Lou, W. Wang, B. Huang and Y. Dai, *Nanoscale*, 2013, **5**, 1870.

59 Z. Pei, L. Ding, H. Lin, S. Weng, Z. Zheng, Y. Hou and P. Liu, *J. Mater. Chem. A*, 2013, **1**, 10099.

5 50 M. Liu, X. Qiu, M. Miyauchi and K. Hashimoto, *Chem. Mater.*, 2011, **23**, 5282.

51 F. Zuo, K. Bozhilov, R. J. Dillon, L. Wang, P. Smith, X. Zhao, C. Bardeen and P. Feng, *Angew. Chem., Int. Ed.*, 2012, **51**, 6223.

52 M. Li, W. Hebenstreit, U. Diebold, A. M. Tyryshkin, M. K. Bowman,

10   G. G. Dunham and M. A. Henderson, *J. Phys. Chem. B*, 2000, **104**, 4944.

53 J. Su, X.-X. Zou, Y.-C. Zou, G.-D. Li, P.-P. Wang and J.-S. Chen, *Inorg. Chem.*, 2013, **52**, 5924.

54 E. Yagi, R. R. Hasiguti and M. Aono, *Phys. Rev. B*, 1996, **54**, 7945.

15 55 N. A. Deskins and M. Dupuis, *Phys. Rev. B*, 2007, **75**, 195212.

56 J. Tang, W. Wang, G.-L. Zhao and Q. Li., *J. Phys.: Condens. Matter.*, 2009, **21**, 205703.

57 V. M. Khomenko, K. Langer, H. Rager and A.Fett, *Phys. Chem. Minerals*, 1988, **25**, 338.

20 58 Y. Matsumoto, M. Murakami, T. Shono, T. Hasegawa, T. Fukumura, M. Kawasaki, P. Ahmet, T. Chikyow, S. Koshihara, H. Koinuma, *Science*, 2001, **291**, 854.

59 S. D. Yoon, Y. Chen, A. Yang, T. L. Goodrich, X. Zuo, D. A. Arena, K. Ziemer, C. Vittoria and V. G. Harris, *J. Phys.: Condens. Matter*,

25   2006, **18**, L355.

60 D. Kim, J. Hong, Y. R. Park and K. J. Kim, *J. Phys.: Condens. Matter*, 2009, **21**, 195405.

61 S. Zhou, E. Čižmár, K. Potzger, M. Krause, G. Talut, M. Helm, J. Fassbender, S. A. Zvyagin, J. Wosnitza and H. Schmidt, *Phys. Rev. B*,

30   2009, **79**, 113201.

62 B. Santara, P. K. Giri, K. Imakita and M. Fujii, *Nanoscale*, 2013, **5**, 5476.

63 X. Zou, G. Li, Y. Zou, P. Wang, J. Su, J. Zhao, Y. Wang and J. Chen, *Acta Chimic Sinica*, 2012, **70**, 1477.

35 64 S. Pan, W. Lu, Y. Zhao, W. Tong, M. Li, L. Jin, J. Y. Choi, F. Qi, S. Chen, L. Fei and S.-F. Yu, *ACS Appl. Mater. Interfaces*, DOI: 10.1021/am4045162 2013.

65 J. Wang, P. Zhang, X. Li, J. Zhu and H. Li, *Appl. Catal. B Environ.*, 2013, **134-135**, 198.

40 66 I. Justicia, P. Ordejón, G. Canto, J. L. Mozos, J. Fraxedas, G. A. Battiston, R. Gerbasi and A. Figueras, *Adv. Mater.*, 2002, **14**, 1399.

67 M. S. Hamdy, R. Amrollahi and G. Mul, *ACS Catal.*, 2012, **2**, 2641.

68 Z. Zhang, M. N. Hedhili, H. Zhu and P. Wang, *Phys. Chem. Chem. Phys.*, 2013, **15**, 15637.